A Hybrid Segmentation Pattern of Partial Transmission in Computer Networks to Reduce the Complexity Level

Rasha Subhi Hameed[1*], Noora Shihab Ahmed[2], Tameem Mohammed Mahmood[3]

[1] Department of Computer Science
University of Diyala, 32001, Diyala, IRAQ

[2] Computer science department, College of Science,
University of Halabja, Kurdistan, Iraq, 46018, Halabja, IRAQ

[3] Al-Yarmouk University Collage, 32001, Diyala, IRAQ

* Corresponding Author

Abstract: Partial transmission sequence (PTS) is seen as a related project in the framework of the Orthogonal Frequency Division Multiplexing (OFDM) to suppress the medium to high Peak-to-Average Power Ratio problem. The PTS chart data is based on dividing the back into subdivisions and their weight by combining step-by-step factors. Despite the fact that PTS can reduce the high specifications. The Computational Complexity Level (CC) limits the scope of application to match PTS use with ground applications. In PTS, there are three main distribution schemes. Interleaving projects (IL-PTS), arbitrary and alternate (PR-PTS) and Ad-PTS. In this paper, another algorithm called the Hybrid Pseudo-Random and Interleaving Cosine Wave Shape (H-PRC-PTS) is presented and the PR-PTS equilibrium is established by stabilizing the cousin waveform between languages (S-IL-C- PTS), which was suggested in the previous work. The results showed that the proposed algorithm could reduce the validity of PAPR as a PR-PTS scheme, although the CC level was significantly reduced.

Keywords: Partial Transmit Sequences, Peak-to-Average Power Ratio, Computational Complexity, Orthogonal Frequency, Division Multiplexing

1. Introduction

Recently, Orthogonal Frequency Division Multiplexing (OFDM) has forced itself to control remote messaging structures due to its high-interest rate for multiple uses of the remote frame. The OFDM structure is known to meet the needs of business sectors, which have not previously been able to manage the remote framework. OFDM has been approved by some remote frameworks because of its interests, for example, instability versus fading [1], instantaneous number of reverse changes (IFFT) [2], depending on the ease of use and the high-speed range of information [3], and the skills of using transfer speeds [4]. Thus, OFDM is used by many remote frameworks such as IEEE.802.11 [5], IEEE.802.15 [6] and IEEE.802.16 [7]. In addition, OFDM is an integral part of communication systems, for example, computer video communication (DVB) [8] and digital television broadcasting (DTVB) [9]. Also, OFDM is a multi (LTE) adaptation method and is a standard for a 4G [10].

Recently, OFDM-based safety has been introduced in Fifth Age technology (5G), for example, as a separate OFDM (F-OFDM) framework [11] and generally as a separate multi-carrier framework (UFMC) [12]. From a point of view, the main drawback of DM is for PPR height [13]. For example, HPAs should help significantly to prevent signal bending. As a result, the difference in HPA specifications indicates a decrease in efficiency and an increase in the cost of the system [14]. Using these methods, PAPR defines some strategies for overcoming the main challenge, for example, incomplete partial transmitted sequence (PTS) [15], clipping techniques [16], reservation (TR) [17], selective level mapping (SLM) [18], installation steps [19].

PTS technique due to the reduction of high PPRR potential without affecting performance on one of the most intelligent methods of reducing high PAPR status considers PTS to share information images from the OFDM framework to some subgroups and the weight of these subgroups by the collection. One of the factors of the stage depends on re-joining. One of the hallmarks of PTS algorithms is the reduction of PAPR credit beyond 3DB. Once again, CCP is a key test for PTS strategy in real applications [20]. This computational weighting burden requires thorough research to distinguish between IFFT recording and the ideal phase factor [21] to locate the best factor.

In the reviewed literature, several efforts have been made to improve PAPR in order to reduce survival and reduce the CC framework in the PTS strategy, including the Varahram's algorithm 2011 [22], which There is another set of step-by-step components to reduce the CC level with a slight decrease in the supply of the count. In addition to the implementation of PAPR, Kim [23] proposed a less CC strategy using the rotating modulation method instead of using gradual rotating elements to create the perfect OFDM signal. Once again, multiple algorithms are provided to participate in regular programs to reduce PAPR skills or reduce CC levels. Most integrated technologies reduce PAPR performance, extend CC levels and other methods. In 1999, Kang [24] introduced another subclass scheme, IL-PTS and PR-PTS. Kang's strategy could greatly reduce CC. Whenever possible, PAPR reduction was not the PR-PTS method at all. In addition, it has lost some of the information it collects, as Kang's technique relies on duplication and combines specific parts of the blocks. Therefore, the frame is low. Miao [25] introduced another technology that can intercept PR-PTS and IL-PTS with a network to block the CC level of the frame. Regardless of Miao's strategy, it can reduce the system of CC, resulting in a deficiency in the PAPR, which in turn reduces productivity.

In addition, Hong [13] proposed a technique to reduce computational complexity by using PR-PTS in half sub-blocks and half of IL-PTS for all other branches. The point of Hong's algorithm is that PAPR has a higher reputation than PR-PTS, and this algorithm requires at least four subdivisions. In [27], Ibraheem proposed another distribution program, combining the on-going Ad-PTS and IL-PTS programs. In this program, PAPR has been halved from IL-PTS and AD PTS, while Ibrahim's plan is limited to AD PTS. In addition, Jawhar introduced another program dedicated to improving PAPR, further reducing performance with ADPTS and ILPTS designs. Similarly, Jahawarr introduced [28] in two programs by promoting PPR reduction. Next program relied on splitting the IL-PTS into two separate networks. Despite the fact that technologies have improved the implementation of in PAPR, scientific estimates are in line with ADPTS maps [29]. Finally, Jahawar [30] updated new plans to improve the IL-PTS by lowering PAPR's value. Jawaha methods rely on the accuracy of the IL-PTS framework for the delivery of new networks, in which marine transmissions are not separated from IL-PTS networks, however, PAPR has been remotely reduced. Accordingly, this article introduces another mixing technique that can reduce the efficiency of PAPR, which aligns the PRPTS coordinate with a massive reduction in CC levels [31], [32].

The rest sections of the study are organized as follows: In Section 2, the OFDM system is described. Then, the PTS technique is analysed in Section 3. Next, Section 4 discusses the conventional partitioning schemes. After that, Section 5 introduces the proposed method. Finally, the results are discussed in Section 6, and the conclusion points are indicated in Section 7.

2. OFDM System

Input data in OFDM are primarily defined by baseband modulation schemes such as QAM. The modulated symbols y_k {k = 0, 1, 2, ..., N-1 will be converted to a time field (TD) using IFFT operations, to produce an OFDM signal for a discrete basis y (n) can be specified by:

$$y(n) = \frac{1}{\sqrt{N}} \sum_{k=0}^{N-1} Y_k e^{j2\pi k \frac{n}{N}} \quad , \quad n = 0, 1, 2, ..., N-1 \tag{1}$$

Where y and N symbolize the number of subcarriers. The OFDM signal for a separate baseband is compatible with the sub-N about the K-test image of the information. In TD, the OFDM signal is used by adding balanced N samples. After that, the instantaneous density of some samples exceeds the normal intensity. This is done when these examples are comparable. The invalidity of this signal means PAPR, and by separation from the extreme power, the average signal strength is generated. PAPR is generally associated with decibels (dB) [33], [34].

$$PAPR = \frac{\max|y(n)|^2}{E\{|y(n)|^2\}} \tag{2}$$

Moreover, due to the possibility of signal transmission outside the PMR due to high PAPR, some parts of the frame, such as HPA are transferred directly to the non-linear area. After that, the superiority of the signals will change, and this indicates degradation in efficiency and withdrawal from the BER implementation [33].

Because PAPR data is used, an additional sampling factor (L) is used to ensure PAPR estimation, given the fact that, for example, it may be lost for a few moments. In this method, the excessive activity provides the properties of comparative properties of separate time signals in permanent time signals. Excessive sampling activity [L-1] can be satisfied by adding N zero to samples [32]. In addition, CCDF generally assesses the likelihood of PAPR values. Used for this purpose, it leaves a certain level of the threshold value (PAPR0).

$$\Pr(PAPR > PAPR_0) = 1 - (1 - \exp(-PAPR_0))^{NL} \tag{3}$$

3. The Conventional PTS (C-PTS)

PTS is a potential strategy that can distort more than 3db in using PRPR without blocking BER execution [20]. The main idea about C-PTS is that it is a barrier to the distribution of information under sub-blocks.

$$Y = \sum_{v=1}^{V} Y_v \tag{4}$$

Where sub-blocks represent the blocks by V. Shortly afterwards, the N-IFFT activity is performed on the sub-blocks to synchronize the information with the following blocks. With the idea of adding zero instead of null and false subcarriers to eliminate N-IFFT length. After that, the TD sub-blocks are copied from many phases of phase (b_v) elements so that input and output sequences can be added. Equation (5) DM is expressed with the signal.

$$y = \text{IFFT}\{\sum_{v=1}^{V} b_v Y_v\} \tag{5}$$

The direct use of IFFT is used to convert b_v to TD based on the fact that a large number of phase revolution factors are placed on one. Using these functions, output the OFDM signal,

$$y = \text{IFFT}\{\sum_{v=1}^{V} b_v Y_v\} \tag{6}$$

Where v = {1, 2, ..., V} and b_v talks about the factors of the phase revolution. Finally, PAPR is computed by the grouping of each applicant, while the next value is chosen with the least respect for PAPR. The OFDM output signal can be used as communication using the PTS method [29],

$$\text{OFDM signal} = \sum_{v=1}^{V} b_v y_v \tag{7}$$

From Fig. 1, it is clear that PTS depends on the distribution and partitioned scheme programs, as described in the next section and phase changes factors, which are usually mandatory bv {{± 1. or {±1, ±j} to decrease the complex multiplications. Once again, the components of the rotation can be achieved

$$b = \{b_v = e^{j 2\pi v / W} \mid v = 0,1,.......,W-1\} \tag{8}$$

Where the value of phase excitation varies as a symbol of W. Ideal phase weight variables can be found using optimization.

$$\{b_1, b_2, \ldots, b_v\} = \arg\min_{1 \le w \le W} \left(\max_{0 \le n \le NL-1} | \sum_{v=1}^{V} b_v y_v | \right) \qquad (9)$$

In C-PTS, the framework needs to do thorough research to determine the ideal phase factor, so this activity imposes a higher CC level and takes more time to process. The transmitter must also be collected as peripheral data (collecting 2 W1 1) to send the information to the receiver [30]. Note that CC PR-PTS and Ad-PTS levels are different from IL-PTS levels because all IFFT steps require processing under the information block in the IFFT unit, although the IL-PTS map requires fewer steps to change. Above the sub-blocks in the TD of the repeat area (FD). Therefore, the amount of IL-PTS does not increase and increases as much as PR-PTS and Ad-PTS, but the loss of PAPR reduces degradation of efficiency. These ideas inspire us to use our method which will be shown in the next section. Fig. 1 shows the block diagram of C-PTS.
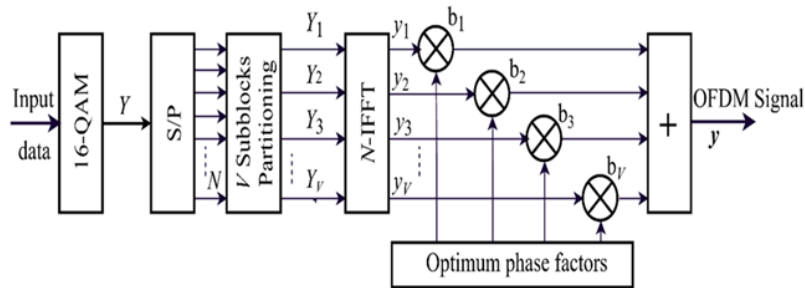

Fig. 1 - C-PTS block diagram [3].

The predominant PAPR threshold in the PR-PTS design is observed by paradoxical designs and other partitions but this component is also included in the higher CC level. However, CCIL PTS has the least regular schedule to mitigate reduced PLR performance. With these lines, a combination of PR-PTS with an IL-PTS section can lead to fewer numerical tasks, however, the process of reducing PAPR and calculating PR-PTS [19], [27] is the opposite. In this paper, the aim is to reduce CC levels without examining PAPR performance. For this purpose, two Division projects have been used, the PR-PTS plan and the S-IL-C-PTS balance plan [18].

4. Conventional Partitioning Scheme

As mentioned earlier, image accuracy is an important development in the PTS method in several subgroups. In this section, the relationship between examples of organizing information is reduced. There are three regular distribution schemes [24]: IL-PTS, Ad-PTS, and adjacent Arbitrary pseudo-random (PR-PTS). The three regular distribution programs can record various demonstrations of PAPR reduction at the CP level. Distribution activity must meet the following conditions: first, the sub-blocks should not be covered and their size should not be equal, second, each subcarrier should be placed under one time only, third, every sub-block must have N\V carriers.

In PR-PTS, N / V sub-carriers are randomly distributed under each block, although the Ad-PTS N / V of successive carriers is gradually allocated below the phases, while the IL-PTS carrier sub-block Assigns everyone inside with a specific interval (V), as shown in Fig. 2.
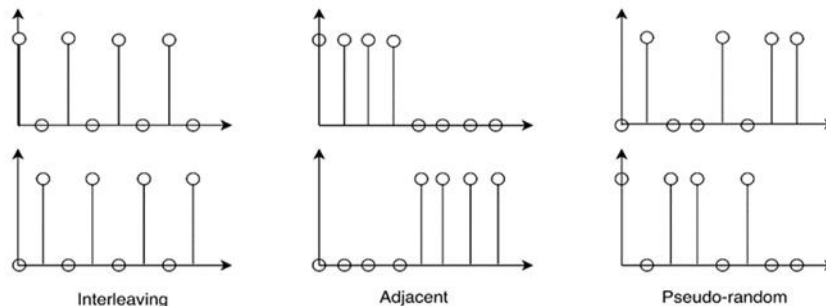

Interleaving   Adjacent   Pseudo-random

Fig. 2 - C-PTS block diagram [3].

Also, between regular schemes, the PR-PTS scheme is considered the best concern about the low PAPR threshold, and then the next best thing is the Ad PTS project scheme. The IL-PTS is considered the most horrible and worse scheme [15]. This difference is a direct result of the PR-PTS and Ad-PTS programs, which have a less automatic correlation between the following barriers. However, due to the revolving nature of this scheme, the relationship between IL-PTS subcarriers is considered high due to the periodic nature [31].

Paradoxically, PR-PTS and Ad PTS have good values in terms of high CC compared level and ILPTS design. PR-PTS and Ad PTS have their own sample TD. They change. However, due to the intermittent nature of the IL-PTS structure, fewer IFFT measures are required to perform test changes in IL-PTS TD. Therefore, the CC level for three subcategory programs can be reported as follows.

- The number of complex additions (c) and complex multiplications ($C_{mult}^{PR/Ad}$) of PR-PTS and Ad-PTS can be formulated as [26]

$$C_{add}^{PR/Ad} = V \left[N \log_2 N \right] \tag{10}$$

and,

$$C_{mult}^{PR/Ad} = V \left[\frac{N}{2} \log_2 N \right] \tag{11}$$

- The number of multiplication operations (C_{mult}^{IL}) and addition operations (C_{add}^{IL}) of the IL-PTS scheme when performing the Cooley-Tukey IFFT algorithm can be formulated as [24],

$$C_{mult}^{IL} = V \left[\frac{N}{2V} \log_2 \frac{N}{V} + N \right] \tag{12}$$

and,

$$C_{add}^{IL} = V \left[\frac{N}{V} \log_2 \frac{N}{V} \right] \tag{13}$$

It should be noted that the CC level of PR-PTS and Ad-PTS differs from that of IL-PTS, as all stages of IFFT must be completed to process the data in the IFFT region, while as are some steps for IL-PTS scheme Requires Converting Frequency Domain (FD) sub-blocks to TD. As a result, the number of IL-PTS additives and additives is lower than PR-PTS and Ad-PTS, but due to a decrease in PAPR. These ideas prompted us to formulate our opinion in the next section.

5. Proposed method

As mentioned above, the high gap of the PAPR band is predicted by the PR-PTS compared to other subunits, however, this element is combined by a larger CC. In any case, IL-PTS has the shortest CC in the normal range in case of PAPR performance decline. In this sense, by combining the parallel blocks of the PR-PTS and IL-PTS divisions, a small number of digitization tasks can be achieved; however, reducing the performance of the PAPR is the degradation and formation of the PR-PTS [26].

In this article, the goal is to reduce the CC level without withdrawing PAPR performance. To this end, two divisions were used; PR-PTS designed produced a waveform wave-shaped scheme chart (S-IL-C-PTS). The strategy suggested in this article is coordination between the PR-PTS scheme and the equivalent S-IL-C-PTS. Similar to these lines, the combined technique is called random wave cosine-wave diagram shape (H-PRC-PTS). The H-PRC-PTS algorithm uses the clear visibility of each scheme without withdrawing a PAPR implementation less than PR-PTS.

5.1. S-LL-C-PTS Scheme

S-IL-C-PTS has been shown to explain the observed increase in PAPR IL-PTS scheme with multivariate form analysis [30]. The S-IL-C-PTS relies on the interaction of the IL-PTS method to form a single line. The S-IL-C-PTS process starts when the column of the IL-PTS is fixed in the SG group and the V part is set for each group, with the addition G = {1, 2, 3, ..., N / V}. From that point on, it was the SG {G = 2, 4, 6, ..., N / V} groups that were selected to prepare. In the background, the second image was generated from the IL-PTS in which the diffraction was used to imitate the 30 waves. To understand the binding of IL-C-PTS, graphs were drawn. The first row of every even group is replaced with the last row while the second row is changed by the row one before the last, and so forth. As a result, another matrix is generated from the IL-PTS matrix is, where the symmetrical distribution of the subcarriers is formed as cosine waves [30]. In order to understand the S-IL-C-PTS scheme, the example below illustrates the S-IL-C-PTS scheme procedure when N= 16, and V= 4. The IL matrix is established first as follow,

$$\text{IL-matrix} = \begin{bmatrix} Y_1 & 0 & 0 & 0 & Y_5 & 0 & 0 & 0 & Y_9 & 0 & 0 & 0 & Y_{13} & 0 & 0 & 0 \\ 0 & Y_2 & 0 & 0 & 0 & Y_6 & 0 & 0 & 0 & Y_{10} & 0 & 0 & 0 & Y_{14} & 0 & 0 \\ 0 & 0 & Y_3 & 0 & 0 & 0 & Y_7 & 0 & 0 & 0 & Y_{11} & 0 & 0 & 0 & Y_{15} & 0 \\ 0 & 0 & 0 & Y_4 & 0 & 0 & 0 & Y_8 & 0 & 0 & 0 & Y_{12} & 0 & 0 & 0 & Y_{16} \end{bmatrix} \tag{14}$$

After that, the IL matrix is partitioned into SG groups, denoted by {S1, S2, S3, S4} groups, as follows:

$$\text{IL-matrix} = \begin{bmatrix} Y_1 & 0 & 0 & 0 & Y_5 & 0 & 0 & 0 & Y_9 & 0 & 0 & 0 & Y_{13} & 0 & 0 & 0 \\ 0 & Y_2 & 0 & 0 & 0 & Y_6 & 0 & 0 & 0 & Y_{10} & 0 & 0 & 0 & Y_{14} & 0 & 0 \\ 0 & 0 & Y_3 & 0 & 0 & 0 & Y_7 & 0 & 0 & 0 & Y_{11} & 0 & 0 & 0 & Y_{15} & 0 \\ 0 & 0 & 0 & Y_4 & 0 & 0 & 0 & Y_8 & 0 & 0 & 0 & Y_{12} & 0 & 0 & 0 & Y_{16} \end{bmatrix} \tag{15}$$

Next, only the even groups {S1, S2} are chosen for processing, where the rows of each even group are exchanged with each other; thus, the S-IL-C matrix can be expressed as,

$$\text{S-IL-matrix} = \begin{bmatrix} Y_1 & 0 & 0 & 0 & 0 & 0 & 0 & Y_8 & Y_9 & 0 & 0 & 0 & 0 & 0 & 0 & Y_{16} \\ 0 & Y_2 & 0 & 0 & 0 & 0 & Y_7 & 0 & 0 & Y_{10} & 0 & 0 & 0 & 0 & Y_{15} & 0 \\ 0 & 0 & Y_3 & 0 & 0 & Y_6 & 0 & 0 & 0 & 0 & Y_{11} & 0 & 0 & Y_{14} & 0 & 0 \\ 0 & 0 & 0 & Y_4 & Y_5 & 0 & 0 & 0 & 0 & 0 & 0 & Y_{12} & Y_{13} & 0 & 0 & 0 \end{bmatrix} \tag{16}$$

Finally, the S-IL-C matrix can be written as,

$$\text{S-IL-C-matrix} = \begin{bmatrix} Y_1 & 0 & 0 & 0 & 0 & 0 & 0 & Y_8 & Y_9 & 0 & 0 & 0 & 0 & 0 & 0 & Y_{16} \\ 0 & Y_2 & 0 & 0 & 0 & 0 & Y_7 & 0 & 0 & Y_{10} & 0 & 0 & 0 & 0 & Y_{15} & 0 \\ 0 & 0 & Y_3 & 0 & 0 & Y_6 & 0 & 0 & 0 & 0 & Y_{11} & 0 & 0 & Y_{14} & 0 & 0 \\ 0 & 0 & 0 & Y_4 & Y_5 & 0 & 0 & 0 & 0 & 0 & 0 & Y_{12} & Y_{13} & 0 & 0 & 0 \end{bmatrix} \tag{17}$$

The known PAPR reduction of S-IL-C-PTS is greater than the IL-PTS, because the autocorrelation observed between IL-PTS subcarriers is higher than the S-IL-C-PTS decrease [16]. Instead, the CC S-IL-C-PTS was determined depending on the segmentation approach and overlap of the Cooley-Tukey IFFT algorithm.

In this way, as in column mapping, all sub-blocks of the S-IL-C-PTS scheme are arranged, where the sub-block V contains the same number of columns and rows. At the same time, if all the sub-blocks are divided into subgroups, the sum of the components is calculated, where a complete subset R = N / V is made, as shown in Table 1. However, the generated signals map each sub-block online according to segmentation and solution approach.

Table 1 - The sub-block arrangement of the S-IL-C-PTS scheme [11]

$v \setminus r$	1	2	…	R
1	Y_1^v	Y_{V+1}^v	…	$Y_{V(R-1)+1}^v$
2	Y_2^v	Y_{V+2}^v	…	$Y_{V(R-1)+2}^v$
…	…	…	…	…
V	Y_V^v	Y_{2V}^v	…	Y_{VR}^v

The size of the rows in Table 1 corresponds to the number of sub-blocks, while R is the size of the subsets in a sub-block. The configuration of the sub-block information in the TD is obtained after using the Cooley-Tukey scheme for each row and section in Table 1. In this way, the TD character can be represented as [11, 23].

$$y_{(q,p)} = \frac{1}{\sqrt{N}} \sum_{v=0}^{V-1} \left\{ W_N^{vq} \left[\sum_{r=0}^{R-1} Y_{v,r} W_R^{rq} \right] \right\} W_V^{vp} \tag{18}$$

($W_N = e^{2j\pi/N}$) is the unrest factor and the components of the p_{th} and q_{th} column are assigned to IFFT y (q, p) mapping. As can be seen from the S-IL-C-PTS scheme methodology, only two rows with active subset carriers are applied to the R-point IFFT-point. Therefore, it can be tightened as part [11].

$$y_{(p,q)} = \frac{1}{\sqrt{N}} \sum_{v=0}^{1} \left\{ W_N^{vq} \left[\sum_{r=0}^{R-1} Y_{(v,r)} W_R^{rq} \right] \right\} W_V^{vp} \tag{19}$$

In S-IL-C-PTS, the computation of IFFT for each sub-block is represented by Equation (19), where the CC can be divided into three parts. Furthermore, the obtained array is read as a row-wise mapping. As a consequence, every single sub-block of S-IL-C-PTS performs two-times R-point IFFT (step-1), N-times complex multiplications (step-2), and R-times of two V-points IFFT (step-3). Therefore, the number of addition operations (C_{mult}^{S-IL-C}) and the multiplication operations (C_{add}^{S-IL-C}) of S-IL-C-PTS when performing the Cooley-Tukey algorithm is:

$$C_{add}^{S-IL-C} = 2N\left[\log_2(\frac{N}{V})+1\right] \tag{20}$$

and,

$$C_{mult}^{S-IL-C} = N\left[\log_2(\frac{N}{V})+V+1\right] \tag{21}$$

It can be seen that the CC of S-IL-C-PTS is higher than that of IL-PTS, but the PAPR reduction gain is improved [30]. Consequently, the S-IL-C-PTS scheme can realize better PAPR reduction gain than that of IL-PTS with slightly increasing of mathematical operations, which motivated us to exploit this prominent feature in the proposed method in this paper.

5.2.   PR-PTS Scheme

As mentioned in section 4, the PR-PTS system is a better algorithm among the standard PAPR performance reduction systems. Assuming that the random distribution of the sub-blocks within the sub-blocks leads to a decrease in the correlation between the sub-blocks [15]. Despite the fact that the PR-PTS algorithm can control PAPR values. A large number of mathematical tasks are considered essential in this process since the PR-PTS system uses the full phase of the IFFT unit while changing the sub-cube. Likewise, PR-PTS technology is the best algorithm when the system structure requires increased PAPR performance.

5.3.   H-PRC-PTS Scheme

As mentioned in the first step of this section, the H-PRC-PTS algorithm combines the PR-PTS scheme and the S-IL-C-PTS scheme to provide a hybrid scheme that can reduce the size of numerical mathematical tasks in general. It also achieves the PAPR, reducing the efficiency equivalent to the PR-PTS scheme design. The H-PRC-PTS technique is recommended to use the high PAPR reduction potential of PR-PTS and the low CC level element of S-IL-C-PTS, where the initial step begins by separating the information symbol Y in two Y into two parts Y_A and Y_B.

$$Y = [Y_1, Y_2, ..., Y_N] \tag{22}$$

So it can also be explained as,

$$Y = [Y_A, Y_B] \tag{23}$$

Here Y_A is the representative of first part of the input data symbol and contains 0.25N or 0.5N or 0.75N of the subcarriers. The second part of the input symbol Y_B can be written as,

$$Y_B = [Y_{(N/2)+1}, Y_{(N/2)+2}, ..., Y_N] \tag{24}$$

After that, the first part YA undergoes the PR-PTS algorithm, in which the YA data sequence is divided into V sub-blocks, and the second part YB undergoes the S-IL-C-PTS algorithm, where the data sequence is partitioned into V sub-blocks,

$$Y_A = \sum_{v=1}^{V} Y_{Av} \tag{25}$$

and,

$$Y_B = \sum_{v=1}^{V} Y_{Bv} \tag{26}$$

Afterwards, the two partitioned parts (Y_A and Y_B) are combined again to produce the hybrid block sequence Y_H,

$$Y_H = [Y_A, Y_B] = [\sum_{v=1}^{V} Y_{Av}, \sum_{v=1}^{V} Y_{Bv}] = \sum_{v=1}^{V} Y_{Hv} \tag{27}$$

Finally, the rest of the C-PTS procedure is performed on H-PRC-PTS, and the minimum PAPR value of the optimum OFDM signal is transmitted to the receiver. Therefore, the output signal of the OFDM can be written as,

$$y = \sum_{v=1}^{V} b_v y_{Hv} \tag{28}$$

where y represents the transmitted OFDM signal.
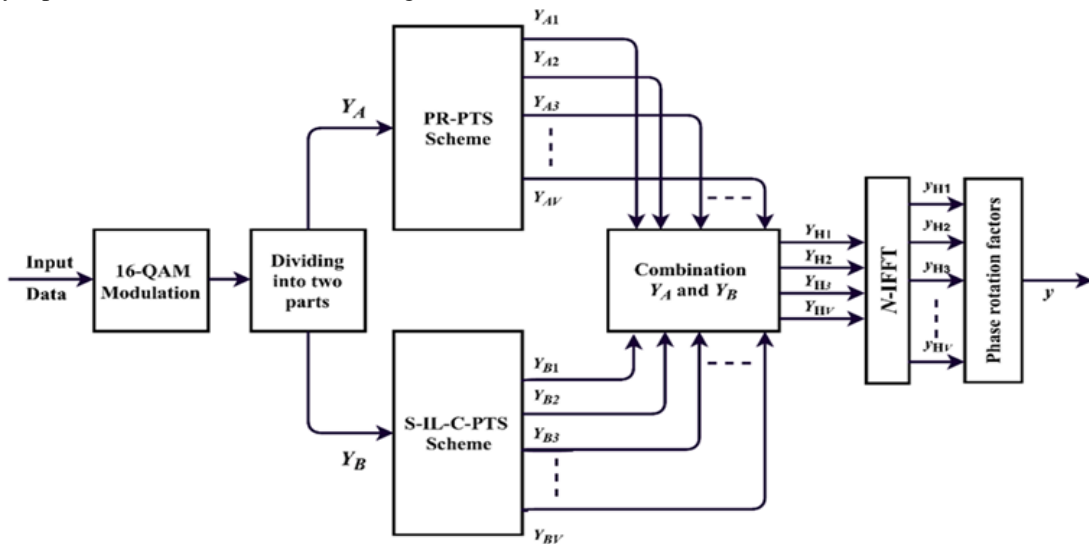
Fig. 3 - H-PRC-PTS scheme block diagram

In the H-PRC-PTS scheme, the initial segment of the algorithm uses the PR-PTS scheme, which can achieve a predominant decrease in the PAPR scheme with a high CC level, while the second piece of the S-IL algorithm is used C- PTS which can achieve a decent reduction of the PAPR scheme with low CC. Since the H-PRC-PTS algorithm can achieve a PAPR reduction efficiency that corresponds to the PR-PTS scheme, this is the best scheme for PAPR reduction in the PTS method. The overall CC level of the system is also reduced.

This is mentioned in the next segment. The number of addition operations ($C_{add}^{H\text{-}PRC}$) and multiplication operations ($C_{mult}^{H\text{-}PRC}$) of the H-PRC-PTS algorithm is the sum of the PR-PTS complexity and the S-IL-C-PTS complexity,

$$C_{add}^{H\text{-}PRC} = V(N' \log_2 N') + 2N'' \left[\log_2(\frac{N''}{V}) + 1 \right] \tag{29}$$

and,

$$C_{mult}^{H\text{-}PRC} = V(\frac{N'}{2} \log_2 N') + N'' \left[\log_2(\frac{N''}{V}) + V + 1 \right] \tag{30}$$

The equation mentioned above represents the number of subcarriers of the initial part (Y_A) and symbolizes the dimensional symbol of the next part (Y_B). The CC level of the H-PRC-PTS algorithm will depend on the number of sub-carriers and since the number of mathematical tasks in the next part (Y_B) implements the S-IL-C-PTS of the sub-carriers, the full CC of the H-PRC-PTS algorithm will not be as large as that of the PR-PTS scheme.

6. Results and Discussion

In this section, the H-PRC-PTS technique is newly created and analysed in a situation which depends on the number of secondary carriers determined in the initial part (Y_A) and in the rear part (Y_B). In this new creation, the first part applies to PR-PTS and the following part to S-IL-C-PTS, with the number of sub-carriers for Y_A and Y_B.

Thus, the number of subset carriers (N', N'') is defined separately (N / 2, N / 2), (N / 4.3N / 4) , (3N / 4, N / 4). In addition, the proposed strategy is compared with the situation PR-PTS. In addition, the parameters used to control the simulations are the number of subcarriers of the N = 256, L = 4 ᵈ 16-QAM to select any 1000 symbols that are rated by CCDF. In addition, V phase coefficients of different sizes are used for this reproduction, sub-blocks W, v they are distinguished as (W, V) to (2, 4), (2, 8), (4, 2), and (4, 4), respectively. CCRR can be summarized as follows from the proposed method PR-PTS strategy [30],

$$CCRR = 1 - \frac{\text{Complexity of H-PRC-PTS}}{\text{Complexity of PR-PTS}} \times 100\% \qquad (31)$$

In these cases, the parameters are set as follows: N rises to 256, sets W and V to (2, 4), (2, 8), (4, 2) and (4, 4) separately. As it stands, the initial portion of Y_A is 0.25N subcarrier, and the remainder of the narrow sub, 0.75N, is distributed in the second part YB. In this case, the proposed policy is called H-PRC2-PTS.

Figure 4 (a) reports the correlation effects of PR-PTS and H-PRC2-PTS, taking into account that W = 2 and V = 4. PR-PTS exceed the H-PRC2-PTS in terms of a PAPR yield of 0.263 dB. Similarly, Figure 4 (b) shows a correlation between PR-PTS and H-PRC2-PTS when W = 2 and V = 8. Clearly, the PR-PTS scheme intersects the H-PRC2-PTS graph by 0.133 dB.

W= 2, and V= 4   W= 2, and V= 8
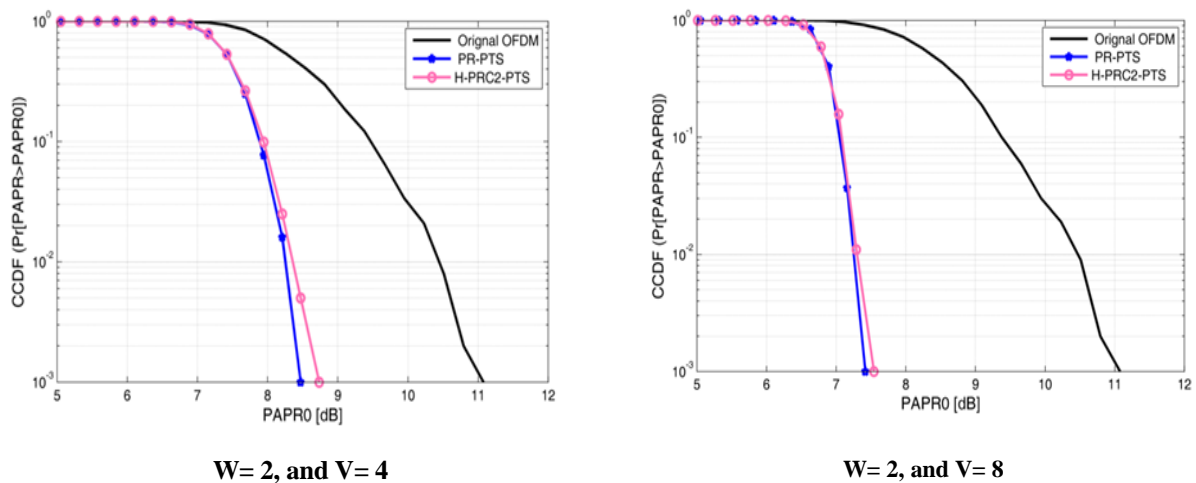
Fig. 4 - Comparison of H-PRC2-PTS and PR-PTS

Figure 5 (a) shows the contrast of the PR-PTS and H-PRC2-PTS algorithm when W = 4 is greater than V = 2. The PR-PTS algorithm violates the H-PRC2-PTS algorithm whenever the output decreases PAPR 0.263 dB. Similarly, Figure 5 (b) shows the difference between PR-PTS and H-PRC2-PTS when W and V are set to 4, where PR-PTS technology overcomes the H-PRC2-PTS method to reduce the PAPR efficiency of 0.263 dB.

| W= 4, and V= 2 | W= 4, and V= 8 |
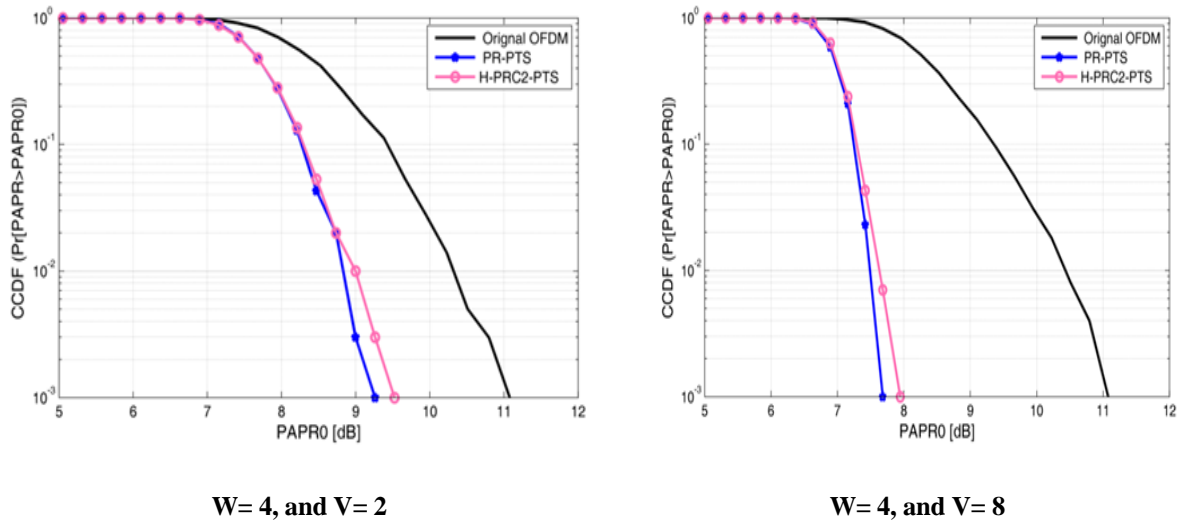
Fig. 5 - Comparison of H-PRC2-PTS and PR-PTS

Similarly, the proposed technology is considered, the performance of PAPR is not as high as the PR-PTS for all levels of W and V, and the CC stage of policy improvement is actually lower, as shown in Table 2.

Table 2 - The Scenario of CCRR

	Scenario ($N/4$, $3N/4$) , $N= 256$					
	PR-PTS		H-PRC2-PTS		CCRR	
(W, V)	C_{mult}	C_{add}	C_{mult}	C_{add}	$CCRR_{mult}$	$CCRR_{add}$
(2, 4)	4096	8192	2800.3	4064.6	31.64%	50.39%
(2, 8)	8192	16384	4144.3	5216.6	49.41%	68.16%
(4, 2)	2048	4096	2224.3	3680.6	---	10.14%
(4, 4)	4096	8192	2800.3	4064.6	31.64%	50.39%

7. Conclusion

The paper proposed a new combination strategy for the C-PTS method in the OFDM framework. The enhanced strategy, H-PRC-PTS, also combines two types of sharing equally, the first is PR-PTS, which provides outstanding PAPR reduction performance with high DC levels, and the second is S-IL-C-PTS, which has adequate CC-level PAPR reduction performance. The results show that the prevalence of the improved technique compared to the best extraordinary segmentation scheme (PR-PTS) compared with the addition of PAPR and CC. Therefore, the new algorithm may be the best combination to control the high CC level of the C-PTS procedure without interrupting the PAPR gain.

Acknowledgement

References

[1] Wang, S.; Da, X.; Chu, Z.; and Liu, J. (2015). Magnitude weighting selection: a method for peak-to-average power ratio reduction in transform domain communication system. IET Communications, 9(15), 1894-1901
[2] Tu, H.C.; and Chiu, C.C. (2007). A novel search method to reduce PAPR of an OFDM signal using partial transmit sequences. International Journal of Communication Systems, 20(2), 147-157
[3] Pejoski, S.; and Kafedziski; V. (2016). Improved Asymptotic Capacity Lower Bound for OFDM System with Compressed Sensing Channel Estimation for Bernoulli Gaussian Channel. Radioengineering, 25(2), 283

[4]   Jawhar, Y.A.; Abdulhasan, R.A., and Ramli, K.N. (2016). Influencing parameters in peak to average power ratio performance on orthogonal frequency-division multiplexing system. ARPN journal of engineering and applied sciences, 11(6), 4322-4332

[5]   Taşpinar, N.; and Bozkurt, Y.T. (2016). PAPR reduction using genetic algorithm in lifting-based wavelet packet modulation systems. Turkish Journal of Electrical Engineering & Computer Sciences, 24(1), 184-195

[6]   Singh, A.; and Singh, H. (2016). Peak to Average Power Ratio Reduction in OFDM System Using Hybrid Technique. Optik, 127(6), 3368-3371

[7]   Jawhar, Y.A.; Abdulhasan, R.A.; and Ramli, K.N. (2016). A new hybrid sub-block partition scheme of PTS technique for reduction PAPR performance in OFDM system. ARPN journal of engineering and applied sciences, 11(6), 3904-3910

[8]   Raja, N.B.; and Gangatharan, N. (2016). A new low complexity DHT based weighted OFDM transmission for peak power reduction. Indian J. Sci. Technol., 9(17), 1-4

[9]   Pachori, K.; and Mishra, A. (2016). An efficient combinational approach for PAPR reduction in MIMO–OFDM system. Wireless Networks, 22(2), 417-425

[10] Anoh, K.; Adebisi, B.; Rabie, K.M.; and Tanriover, C. (2017). Root-based Nonlinear Commanding Technique for Reducing PAPR of Preceded OFDM Signals. IEEE Access, 6, 4618-4629

[11] Zhang, L.; Ijaz, A.; Xiao, P.; Molu, M. M.; and Tafazolli, R. (2017). Filtered OFDM systems, algorithms, and performance analysis for 5G and beyond. IEEE Transactions on Communications, 66(3), 1205-1218

[12] Liu, Y.; Chen, X.; Zhong, Z.; Ai, B.; Miao, D.; Zhao, Z.; & Guan, H. (2017). Waveform design for 5G networks: Analysis and comparison. IEEE Access, 5, 19282-19292

[13] Muller, S.H.; and Huber, J.B. (1997). A novel peak power reduction scheme for OFDM. Proceedings of eighth International Symposium on Personal, Indoor and Mobile Radio Communications-PIMRC'97. Helsinki, Finland, 1090-1094

[14] Wu, X.; Wang, J.; Mao, Z.; and Zhang, J. (2010). Conjugate Interleaved Partitioning PTS Scheme for PAPR Reduction of OFDM Signals. Circuits, Systems and Signal Processing, 29(3), 499-514

[15] Jawhar, Y.A.; Audah, L.; Taher, M.A.; Ramli, K.N.; Shah, N.S. M.; Musa, M.; and Ahmed, M. S. (2019). A review of partial transmit sequence for PAPR reduction in the OFDM systems. IEEE Access, 7, 18021-18041

[16] Taher, M.A.; Mandeep, J.S.; Ismail, M.; Samad, S.A.; & Islam, M.T. (2014). Reducing the power envelope fluctuation of OFDM systems using side information supported amplitude clipping approach. International Journal of Circuit Theory and Applications, 42(4), 425-435

[17] Liang, H.; Chu, H.C.; and Lin, C.B. (2016). Peak- to- average power ratio reduction of orthogonal frequency division multiplexing systems using modified tone reservation techniques. International Journal of Communication Systems, 29(4), 748-759

[18] Taher, M.A.; Singh, M.J.; Ismail, M.; Samad, S.A.; Islam, M.T.; and Mahdi, H. F. (2015). Post-IFFT-modified selected mapping to reduce the PAPR of an OFDM system. Circuits, Systems, and Signal Processing, 34(2), 535-555

[19] Jeng, S.S.; Chen, J.M.; and Chang, P.H. (2011). A low- complexity companding technique using Padé approximation for PAPR reduction of an OFDM system. International Journal of Communication Systems, 24(11), 1467-1479

[20] Al-Jawhar; Y.A.; Ramli, K.N.; Mustapha, A.; Mostafa, S.A.; Shah, N.S.; and Taher, M. A. (2019). Reducing PAPR with Low Complexity for 4G and 5G Waveform Designs. IEEE Access, 7, 97673-97688

[21] Ramli, K.; Taher, M.; Audah, L.; Shah, N.S.; Ahmed, M.; and Hammoodi, A. (2018). An enhanced partial transmit sequence based on combining Hadamard matrix and partitioning schemes in OFDM systems. International Journal of Integrated Engineering, 10(3)

[22] Varahram, P.; and Ali, B.M. (2011). A low Complexity Partial Transmit Sequence for Peak to Average Power Ratio Reduction in OFDM Systems. Radio engineering, 20(3), 677-682

[23] Kim, K.H. (2016). On the Shift Value Set of Cyclic Shifted Sequences for PAPR Reduction in OFDM Systems. IEEE Transactions on Broadcasting, 62(2), 496-500

[24] Shawqi, F. S., Audah, L., Mostafa, S. A., Gunasekaran, S. S., Baz, A., Hammoodi, A. T., ... & Alhakami, W. (2020). A New SLM-UFMC Model for Universal Filtered Multi-Carrier to Reduce Cubic Metric and Peak to Average Power Ratio in 5G Technology. *Symmetry*, *12*(6), 909

[25] Miao, L.; and Sun, Z. (2013). PTS algorithm for PAPR suppression of WOFDM system. Proceedings of the First International Conference on Mechatronic Sciences, Electric Engineering and Computer (MEC). Shengyang, China, 1144-1147

[26] Hong, C.; Qin, Q.; and Chao, T. (2013). An PTS optimization algorithm for PAPR reduction of OFDM system. Proceedings of The First International Conference on Mechatronic Sciences, Electric Engineering and Computer (MEC). Shengyang, China, 3775-3778

[27] Ibraheem, Z.T.; Rahman, M.M.; Yaakob, S.N.; Razalli, M.S.; Salman, F.; and Ahmed, K.K. (2014). PTS method with combined partitioning schemes for improved PAPR reduction in OFDM system. Indonesian Journal of Electrical Engineering and Computer Science, 11(12), 7845-7853

[28] Ramli, K.N.; Taher, M.A.; Shah, N.S.; Audah, L.H.; and Ahmed, M.S. (2018). A New Subblock Segmentation Scheme in Partial Transmit Sequence for Reducing PAPR Value in OFDM Systems. International Journal of Integrated Engineering, 10(8)

[29] Jawhar, Y.; Shah, N.S.; Taher, M.A.; Ahmed, M.S.; Ramli, K.N.; and Abdulhasan, R. (2017). A low PAPR performance with new segmentation schemes of partial transmit sequence for OFDM systems. IJAAS International Journal of Advanced and Applied Sciences, 4(4), 14-21

[30] Al-Jawhar, Y.A.; Shah, N.S.; Taher, M.A.; Ahmed, M.S.; and Ramli, K.N. (2016). An enhanced partial transmit sequence segmentation schemes to reduce the PAPR in OFDM systems. International Journal of Advanced Computer Science and Applications (IJACSA), 7(12), 66-75

[31] Fadel, A. H., Razzaq, H. H., & Mostafa, S. A. (2020). A low complexity partial transmit sequence approach based on hybrid segmentation scheme. *Bulletin of Electrical Engineering and Informatics*, *9*(6), 2371-2379

[32] Mostafa, S. A., Mustapha, A., Shamala, P., Obaid, O. I., & Khalaf, B. A. (2020). Social networking mobile apps framework for organizing and facilitating charitable and voluntary activities in Malaysia. Bulletin of Electrical Engineering and Informatics, 9(2), 827-833

[33] Hung, H.L. (2011). Using evolutionary computation technique for trade-off between performance peak-to average power ration reduction and computational complexity in OFDM systems. Computers & Electrical Engineering, 37(1), 57-70

[34] Jubair, M. A., Mostafa, S. A., Muniyandi, R. C., Mahdin, H., Mustapha, A., Hassan, M. H., ... & Mahmood, A. J. (2019). Bat optimized link state routing protocol for energy-aware mobile ad-hoc networks. *Symmetry*, *11*(11), 1409